RECOGNITION OF THE MINERALOGICAL COMPOSITION OF A HAPLIC PLANOSOLO THROUGH SPECTRORADIOMETRY

André Lima da Silva
Centro de Engenharias, Universidade Federal de Pelotas
São Paulo – São Paulo
http://lattes.cnpq.br/5644601948855467

José Maria Filippini-Alba
Environmental Planning Laboratory, Brazilian Agricultural Research Corporation
Pelotas – Rio Grande do Sul
http://lattes.cnpq.br/2307750005842511

Viter Magalhães Pinto
Centro de Engenharias, Universidade Federal de Pelotas
Pelotas – Rio Grande do Sul
http://lattes.cnpq.br/2659542280394218

Abstract: This work presents a study on the identification of the mineralogical composition of soil by using reflectance spectroradiometry. For this, we have used reflectance data obtained for 49 samples of a haplic planosol located in the Experimental Station Terras Baixas at Capão do Leão, Rio Grande do Sul state. Additionally, these data were processed using the continuum removal technique and the resulting spectral signatures were compared to the reference values found in the literature. Results of this comparison indicated that the spectral signatures of the soil showed absorption features predominantly related to kaolinite, muscovite, wood fragments, and dry vegetation. Specifically, concentrations were observed varying between 30.10% and 57.09% for the element kaolinite with low crystallinity, between 32.40% and 34.19% for muscovite, 37.48% corresponding to wood fragments, and between 32.43% and 42.91% corresponding to dry vegetation. Finally, it was concluded that the technique used was effective in estimating the mineralogical composition of the soil and can be reliably applied in future studies.

Keywords: Reflectance spectroradiometry; Planosols; Mineral composition.

INTRODUCTION

Reflectance spectroradiometry is a technique that quantifies the interaction of terrestrial objects (e.g. rocks, water, vegetation, soil) with electromagnetic radiation in terms of reflected, transmitted and absorbed energy. (FILIPPINI-ALBA, 2007; NOVO, 2008). Thus, this technique allows analyzing the spectral characteristics of radiating objects in order to estimate their various chemical and physical properties. In this sense, each terrestrial target presents different spectral responses, depending on the wavelength range considered (e.g. ultraviolet, visible, infrared, among others). Therefore, the spectral responses of soils estimated using reflectance spectroradiometry are directly associated with their chemical, biological, physical and mineralogical composition. (SOUSA-JUNIOR et al., 2008).

Soil spectroradiometry consists of analyzing the reflectance of soil samples both collected and in situ, with the objective of estimating several characteristics, such as the concentration of a given mineral and the content of other elements. In addition, several authors of studies using reflectance spectroradiometry for edaphic characterization demonstrate that this technique is effective in identifying minerals present in soil samples. (NGUYEN et al., 1991; VISCARRA-ROSSEL et al., 2006; FANG et al., 2018). Thus, the authors state that reflectance spectroradiometry allows obtaining information about soil characteristics in a fast and non-invasive way. Finally, despite being a relatively recent line of research, studies of soil parameters using spectral reflectance data have also proved to be an important tool in precision agriculture, which aims at the efficient and conscious use of soil for cultivation.

Therefore, this study is motivated to contribute to the understanding of the relationship between the behavior of spectral reflectance and different minerals, serving as a tool for the scientific study of extensive areas of soil.

METHODOLOGY

CHARACTERIZATION OF THE STUDY AREA

The study area is located at the Terras Baixas Experimental Station (EETB), of Embrapa Clima Temperado, located in the Municipality of Capão do Leão – RS, as can be identified in figure 1. soils in the lower right quadrant.

According to Filippini-Alba (2007), this area comprises a region characterized as low altitude (~10 m), with a drainage profile

classified as "bad". It is a sandy eutrophic haplic planosol with moderate A horizon and sandy/clay texture, derived from sediments from the Quaternary period. (FILIPPINI-ALBA et al., 2019). The authors also state that the region has primary vegetation of the subtropical grassland type. Finally, the land has as main use the cultivation of rice in a no-tillage system (conservation of straw), with alternations to pasture in periods of 2-3 years, in the case of a poorly drained soil where there is no evidence of erosion.

COLLECTION OF SAMPLES AND SPECTRORADIOMETRIC MEASUREMENTS

Using a cutting shovel, samples were collected in the study area, where portions of soil were extracted in a mesh of 7 x 7 sampling points, at depths of 0-10 cm and 10-20 cm. Thus, 7 transects were determined, where 7 sample points with 15 m spacing were collected, totaling 49 sampling points. In addition, the sampling grid was adjusted with the aid of a total station and a topographic GPS receiver. It must be noted that the sample collection and preparation procedure can be found in more detail at Filippini-Alba et al. (2020).

After collection, the soil samples went through the drying and sieving process, being reduced to a fraction of less than 2 mm. Then, spectroradiometric measurements were performed using a FieldSpec 3 portable ER equipment. For these measurements, only samples obtained between 10 and 20 cm deep were selected, according to the procedure described in Sousa Júnior et al. (2011). Thus, spectroradiometric measurements were performed in a range of wavelengths ranging from 350 nm to 2500 nm, with a spectral resolution of 1 nm. Specifically, measurements were performed by positioning the tip of the ER sensor approximately 10 cm away from each sample, using a halogen light source and calibration performed using a Spectralon reference plate (~100% reflectance). Three reflectance measurements were performed on each sample, allowing the generation of soil spectral reading graphs.

DATA PROCESSING

Spectroradiometer data were processed using The Spectral Geologist (TSG) software to obtain reflectance values for each of the 49 samples. These parameters were analyzed in the form of graphs containing the spectral reflectance curves of the soil samples, in which it is possible to observe different properties, such as albedo, noise and absorption features. (PONTUAL et al., 2008). In this context, the features are associated with the chemical, physical and mineralogical characteristics of the analyzed materials and are useful in the identification of minerals through comparison with reference values.

The spectral curves of the samples were analyzed using the continuum removal technique, which is a simple procedure that allows to accentuate features, reduce external effects and identify elements present in the samples. (CLARK e ROUSH, 1984). By removing the continuum, the spectral curves of the samples are normalized with reference to a common baseline that represents the trend of larger-scale variations observed in the spectral curve. It is noteworthy that this baseline must be tangent to the spectral curve and unite as many points as possible from each reflectance curve close to 1nm.

After performing the continuum removal, the intensities of the absorption features observed in the samples were estimated using the concept of absorption depth described in Meneses e Almeida (2012). For this, Equation 3.1 was used:

$$D = 1 - R', \qquad (3.1)$$

where D is the depth of the absorption band
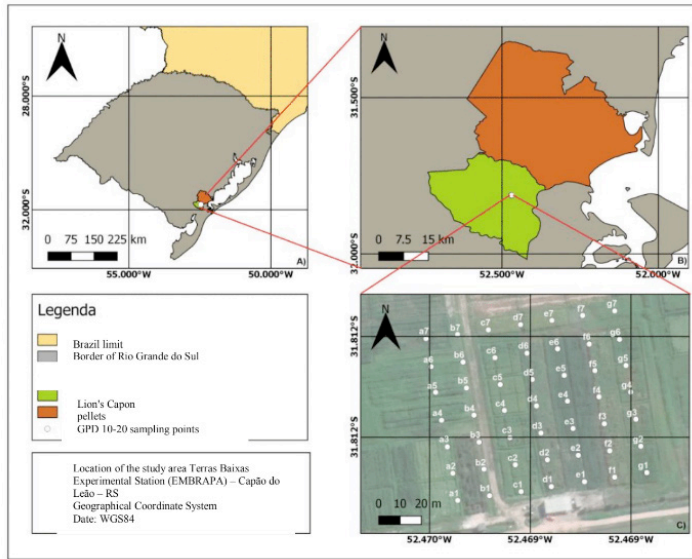
Figure 1 – Location map of the study area in the state, municipal and local context (experimental design).

Source: Author's production.
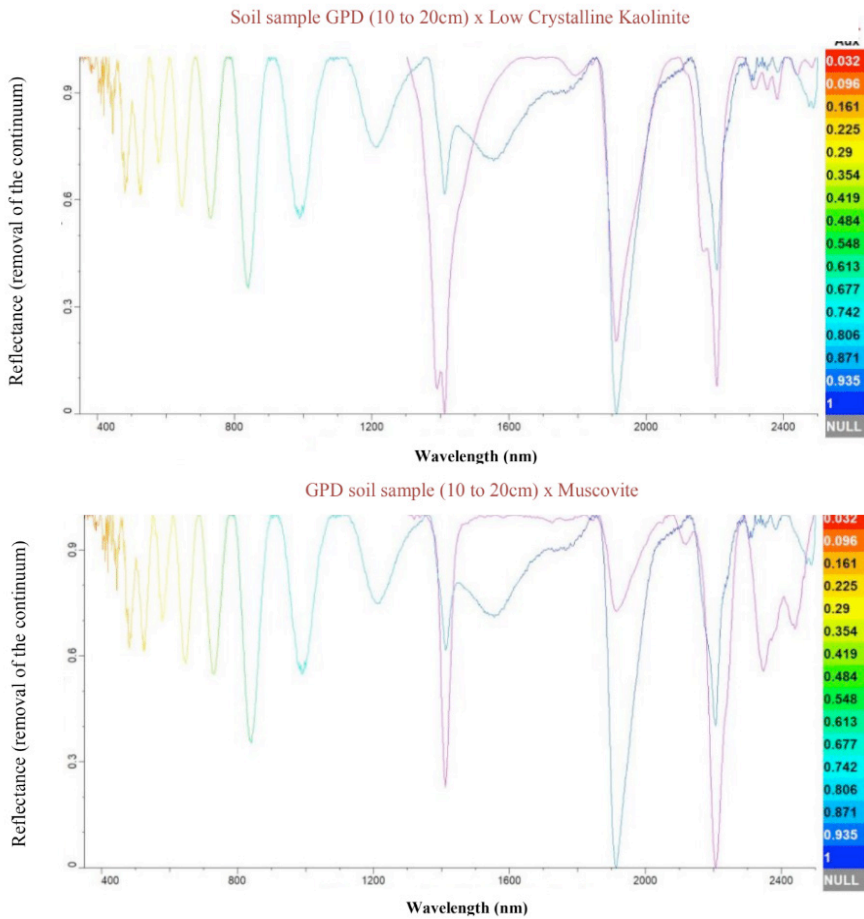
Figure 2 – Comparison of the kaolinite and muscovite spectrum with the spectral signatures of the samples to estimate the proportion of these elements. The color bar represents the variation in the intensity of the spectral signatures in relation to the total weight of the samples.

Source: Author's production.

and R' is the reflectance value corresponding to the absorption point in the spectrum with the continuum removed.

After determining the intensities of the features, the values of each of the samples were compared to the references found in the literature (PONTUAL, 2008; MENESES et al, 2019). This comparison is necessary to identify the minerals/elements present in each of the samples and to estimate the proportions through the intensity of the spectral signatures observed.

Figure 2 illustrates an example of a comparison between the characteristic spectral signatures of kaolinite and muscovite together with the reflectance curves of all samples used.

Table 1 presents some of the reference values used for the diagnosis of absorption features referring to each of the elements identified in the samples used in this study.

RESULTS AND DISCUSSIONS
SPECTRAL ANALYSIS OF SOIL SAMPLES

Figure 3 shows graphs of wavelength variation versus reflectance for all samples. Specifically, this figure illustrates the stacking of spectral signature curves for each of the 49 soil samples studied. In these, the wavelengths of the absorption features are identified for each of the four elements analyzed (kaolinite, muscovite, wood fragments and dry vegetation).

In summary, the spectral signatures of the samples were analyzed using the TSG Core software, in which absorption features predominantly referring to kaolinite, muscovite, wood fragments and dry vegetation were identified. Then, the wavelengths were compared to the reference values found in the bibliography, for later estimation of the proportion of each element in relation to the total weight of the sample. (PONTUAL, 2008; MENESES et al., 2019).

COMPOSITION OF SOIL SAMPLES

The absorption features of each sample were analyzed using the TSG Core software, through which the analyzes were performed considering the elements of interest, together with the reference values presented in Table 1. Thus, the intensity of the features present in each sample was compared to reference values to estimate the proportion of each element in the total weight of the sample. Starting from the verification of these data, the average percentage values of the concentrations of each element were obtained considering all the samples. However, it was observed that not all samples presented the simultaneous occurrence of the four elements studied: kaolinite, muscovite, wood and dry vegetation. Therefore, the samples were organized into three groups to better analyze the concentrations of each element in relation to the average of the group of samples.

Figure 4 shows the vertical bar graph of the average concentration of kaolinite, muscovite, wood fragments and dry vegetation present in the samples from Group 1.

Figure 5 shows the vertical bar graph of the average concentration of kaolinite, muscovite, wood fragments and dry vegetation present in the samples from Group 2.

Figure 6 shows the vertical bar graph of the average concentration of kaolinite, muscovite, wood fragments and dry vegetation present in the samples from Group 3.

Through these results, the proportion of the main components of the samples of each group was quantified:

- Group 1: 30.10% low crystallinity kaolinite, 32.40% muscovite and 37.48% wood fragments. In this group, the occurrence of dry vegetation was not observed.

- Group 2: showed 33.40% of low

Element	Diagnostic absorption features	
	Pontual, 2008	Meneses et al, 2019
Kaolinite	3 features between 2300 and 2400nm; diagnostic double absorption of AlOH between 2160 and 2210 nm.	970f; 1403-1413F (pair); 1810md; 1915f; 2169inf – 2205F; 2311f; 2355f; 2381f
Muscovite	2 absorption features at 2345 and 2435 nm. Absorption to water at 1910 nm weak to absent.	900f; 1139md; 1410mF; 1912f; 2119f; 2205mF; 2346f; 2435f
	TSG Manual	
Wood	500–700 nm (low) 750–1000 nm (high)	
	Zhang et al, 2006	
dry vegetation	1650, 2100 nm and 2300 nm	

where f: weak, md: moderate, F: strong, mF: very strong and inf: inflection.

Table 1 – Reference values used for the diagnosis of absorption features.

Source: Author's production.
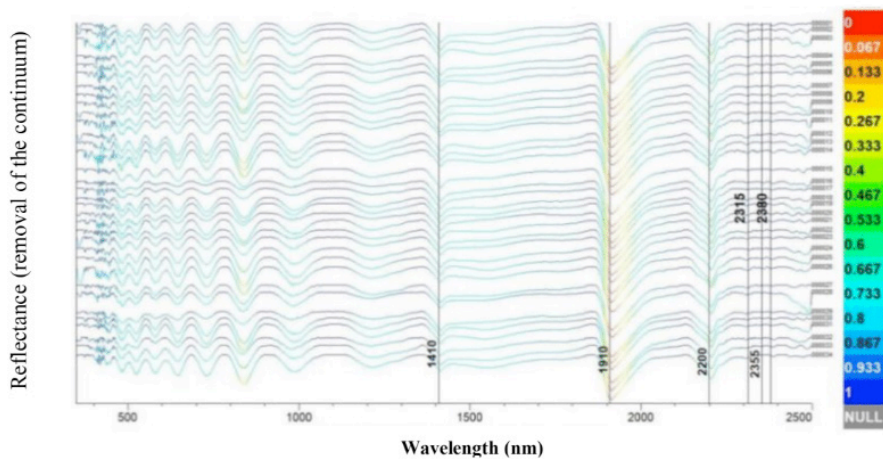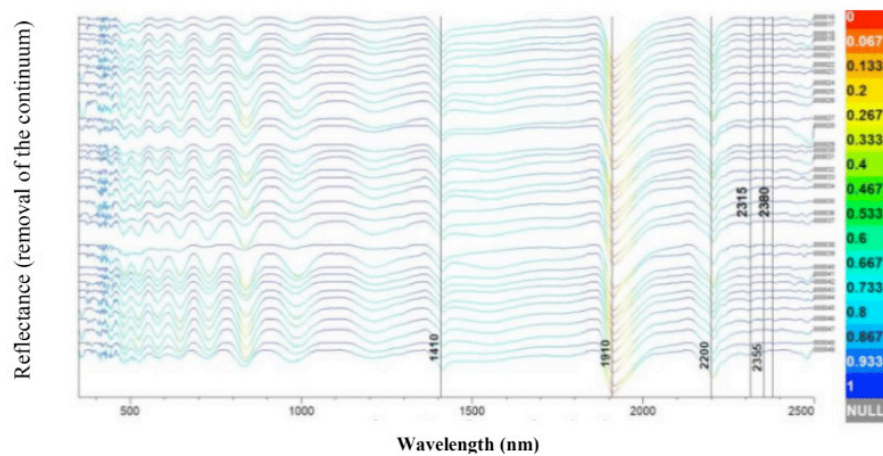
Figure 3 – Wavelength graphs relative to the reflectances of the studied soil samples. The vertical lines indicate the absorption features associated with the elements studied (kaolinite, muscovite, wood fragments and dry vegetation). The color bar represents the variation in the intensity of the spectral signatures in relation to the total weight of the samples.

Source: Author's production.

Average composition of soil samples
GPD (10 to 20 cm - Group 1)
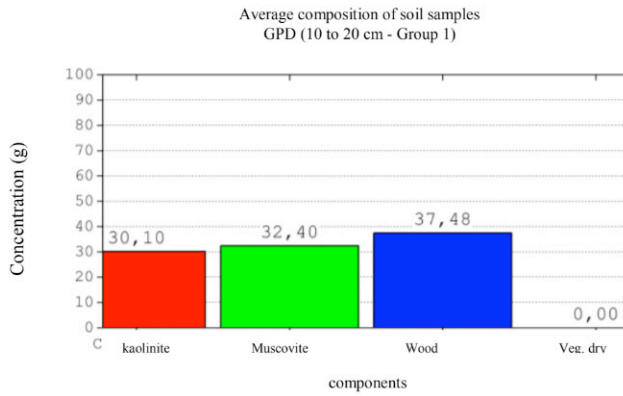
Figure 4 – Mean concentrations of kaolinite, muscovite, wood fragments and dry vegetation present in the samples from Group 1.

Source: Author's production.

Average composition of soil samples
GPD (10 to 20 cm - Group 2)
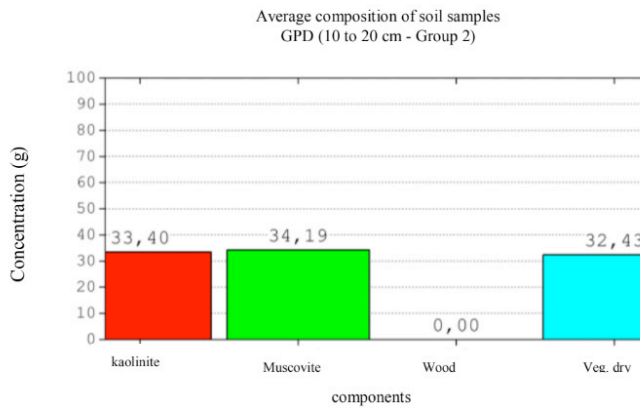
Figure 5 – Mean concentrations of kaolinite, muscovite, wood fragments and dry vegetation present in the samples from Group 2.

Source: Author's production.

Average composition of soil samples
GPD (10 to 20 cm - Group 3)
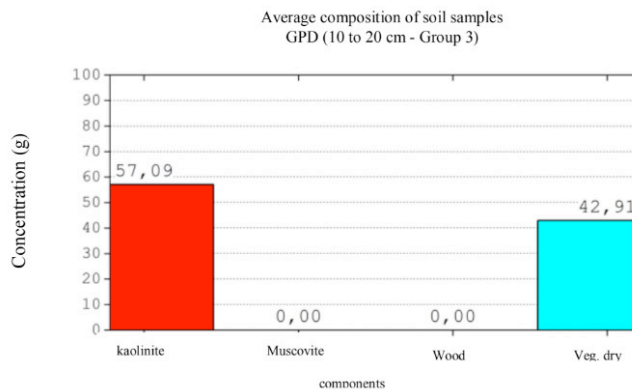
Figure 6 – Mean concentrations of kaolinite, muscovite, wood fragments and dry vegetation present in the samples from Group 3.

Source: Author's production.

crystallinity kaolinite, 34.19% of muscovite and 32.43% of dry vegetation. In this group, the occurrence of wood fragments was not observed.

- Group 3: presented 57.09% of low kaolinite and 42.91% of dry vegetation. In this group, the occurrence of other elements was not observed.

Therefore, it is noteworthy that these results indicate the dominant presence of the kaolinite mineral in the studied soil, but with a similar proportion of muscovite.

Figures 7, 8 and 9 present sector graphs illustrating the distribution of the proportions of kaolinite (red sector), muscovite (green sector), wood fragments (dark blue sector) and dry vegetation (light blue sector) present in the samples of each group.

Starting from figures 7, 8 and 9, it was observed that the proportions of muscovite are predominant in relation to the total weight of the sample in 52.8% of the samples. Wood fragments correspond to the dominant element in 27.8% of the samples, followed by muscovite (13.9% of the samples) and dry vegetation (5.6% of the samples).

Therefore, it can be stated that 52.8% of the soil samples had a high content of kaolinite and 13.9% of the samples had a high content of muscovite.

STATISTICAL ANALYSIS OF THE COMPOSITION OF SOIL SAMPLES

With the objective of evaluating the sampling statistical deviation of the proportion of each element in relation to the mean, the percentage variation of the concentrations calculated for each of the samples was calculated. This variable was obtained through the following equation (PICANÇO, 2019):

$$VP = \sqrt{\left(\frac{q_{sample} - q_{average}}{q_{average}}\right)^2}$$

where VP corresponds to the percentage change in the concentration of a given element in a sample with respect to its mean, q_{sample} is the concentration of the element in a sample and $q_{average}$ is the average concentration of the same element considering all samples. This way, the closer the VP value is to zero, the closer the concentrations of each element in each sample will be to its average value. (PICANÇO, 2019).

Figure 10 shows the VP graph of the concentrations in each sample in relation to the mean values, considering the following elements: kaolinite (red symbols), muscovite (green symbols), wood fragments (dark blue symbols) and dry vegetation (symbols in light blue). It is noteworthy that this analysis was performed considering the averages of each group of samples.

From Figure 10, it can be seen that the kaolinite and muscovite concentrations show some variability in samples 5, 11, 17, 18, 20 and 25, but in general tend to remain close to the mean, since the VP value remains low in most samples. On the other hand, wood and dry vegetation concentrations showed high variability in relation to the average in all samples, which may be directly linked to the form of land use and vegetation density.

DISTRIBUTION OF MINERALS IN THE STUDY AREA

In order to evaluate the kaolinite and muscovite content in the studied soil, maps of mineral distribution were generated, having as a starting point the results presented in the section on composition of the soil samples.

In this context, figures 11 and 12 present, respectively, maps of distribution of kaolinite and muscovite in the study area, where the color bars represent the proportion of the weight of the samples that corresponds to that mineral, as determined by the methods presented in Chapter 3 Both maps were
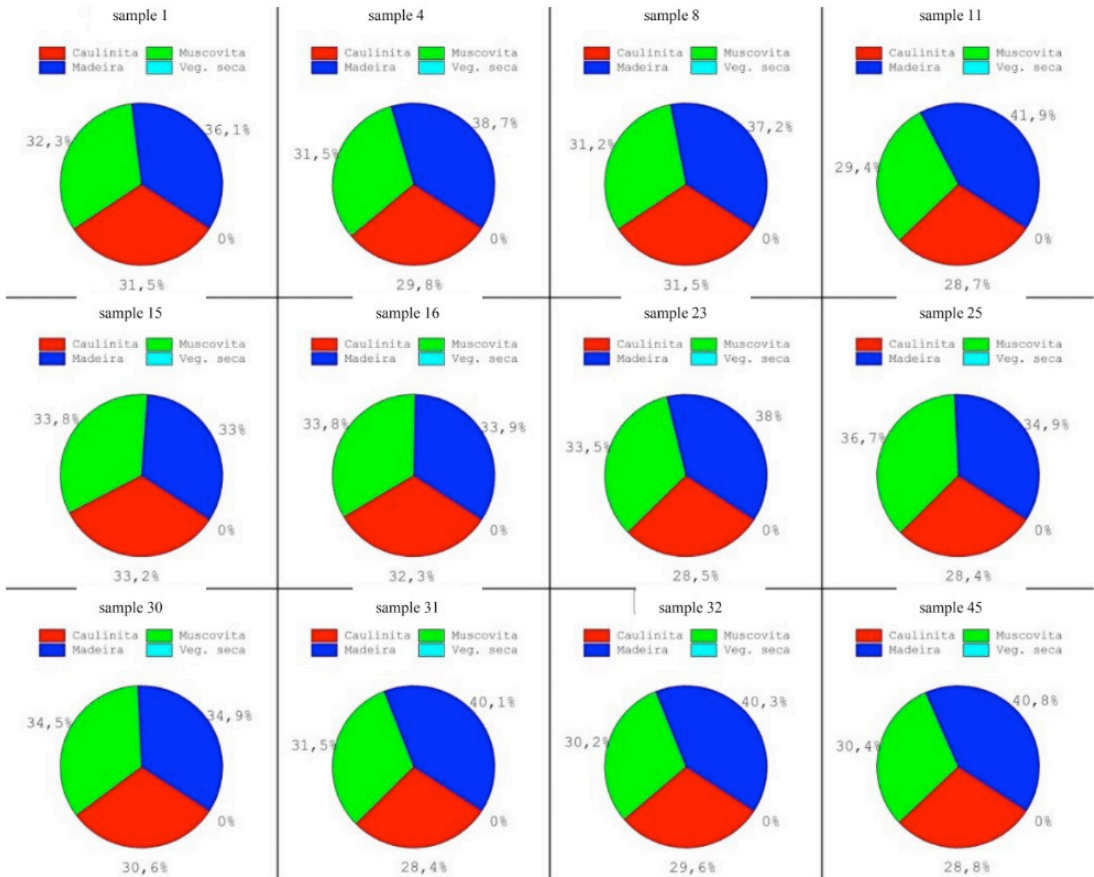
Figure 7 – Concentrations of kaolinite, muscovite, wood fragments and dry vegetation present in the samples from Group 1.

Source: Author's production.
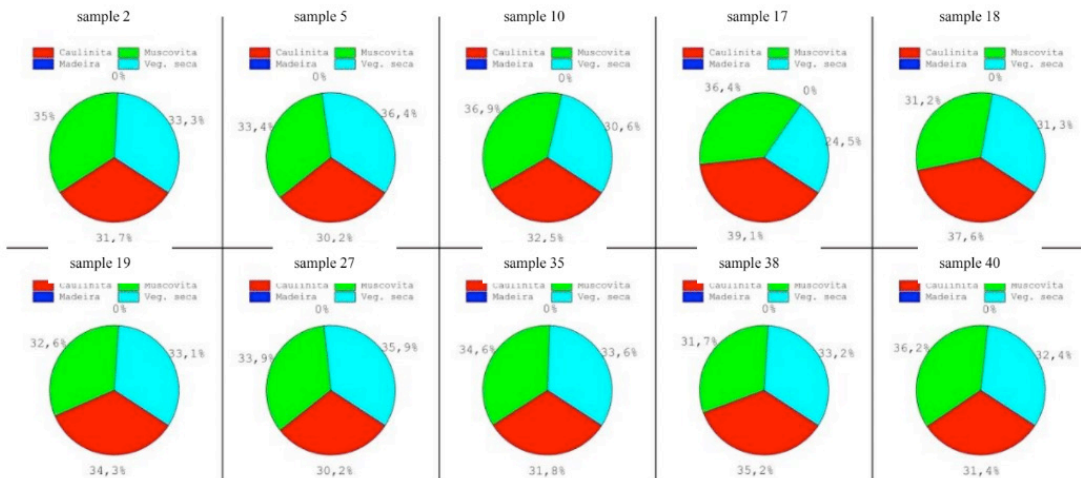
Figure 8 – Concentrations of kaolinite, muscovite, wood fragments and dry vegetation present in the samples from Group 2.

Source: Author's production.
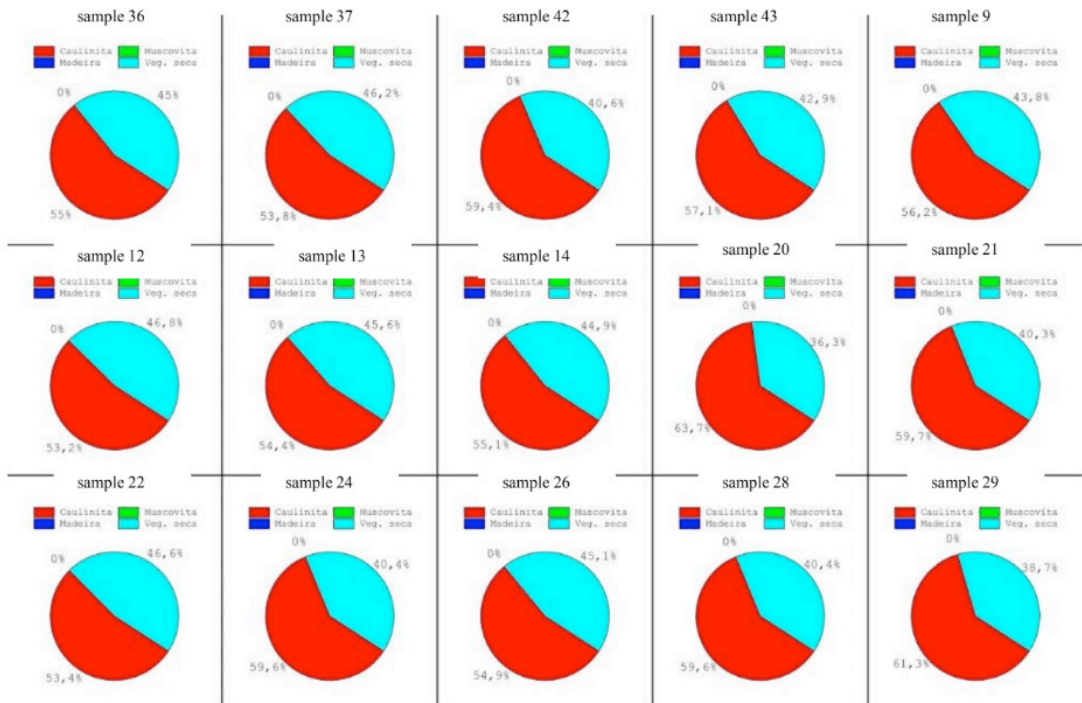
Figure 9 – Concentrations of kaolinite, muscovite, wood fragments and dry vegetation present in the samples from Group 3.

Source: Author's production.
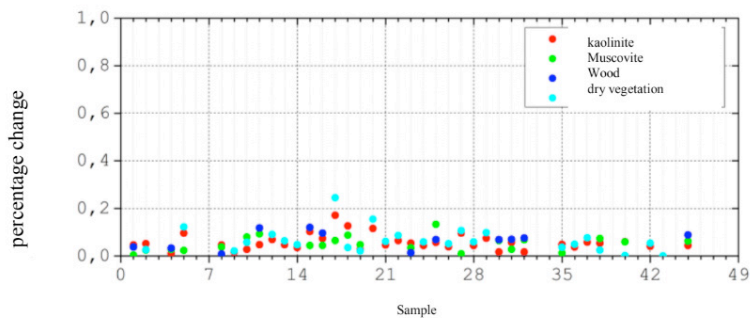
Figure 10 – Percentage variation in the concentration of kaolinite, muscovite, wood fragments and dry vegetation in relation to the average of all samples.

Source: Author's production.

interpolated using the Kernel interpolation method (SILVA, 2015).

From the results presented in Figure 11, it is observed that the soil of the southeast and northwest regions of the study area has the highest kaolinite contents. In this sense, it is important to emphasize that kaolinites are clay minerals that do not exhibit physical-chemical expansibility, so the reduced distance between the structural layers makes it difficult for water to enter the soil, resulting in weak surface adsorption. (PEREIRA, 2004).

From the results presented in Figure 12, it is observed that the soil of the southwest, south and central regions of the study area has the highest levels of muscovite. Since muscovite acts as a clay former and a source of potassium in the soil, it can be said that these regions are associated with the initial phases of mineralogical transformations that result in the formation of kaolinite and other clay minerals. (CARVALHO, 2013).

Figure 13 shows a map with symbols indicating the dominance of kaolinite (red symbols) or muscovite (blue symbols) in the weight of the analyzed samples.

In summary, it can be said that the Capão do Leão region comprises a soil with a certain degree of weathering, however, with the occurrence of points where the process is in its initial stages. This can be evidenced by the results presented in figure 13, where the map indicates that kaolinite is identified as the main mineral in the soil, but muscovite also appears as a predominant and/or subordinate mineral in a considerable amount of the analyzed samples.

CONCLUSIONS

The study showed how chemical, physical and mineralogical characteristics of the soil influence its spectral behavior, allowing the identification of its composition and can be performed automatically through the TSG Core™ software. However, the software did not present high reliability to its results, requiring a manual analysis using other sources of spectral libraries to check the results. Still, spectroradiometrics can be considered an effective and low-cost way to estimate soil attributes.
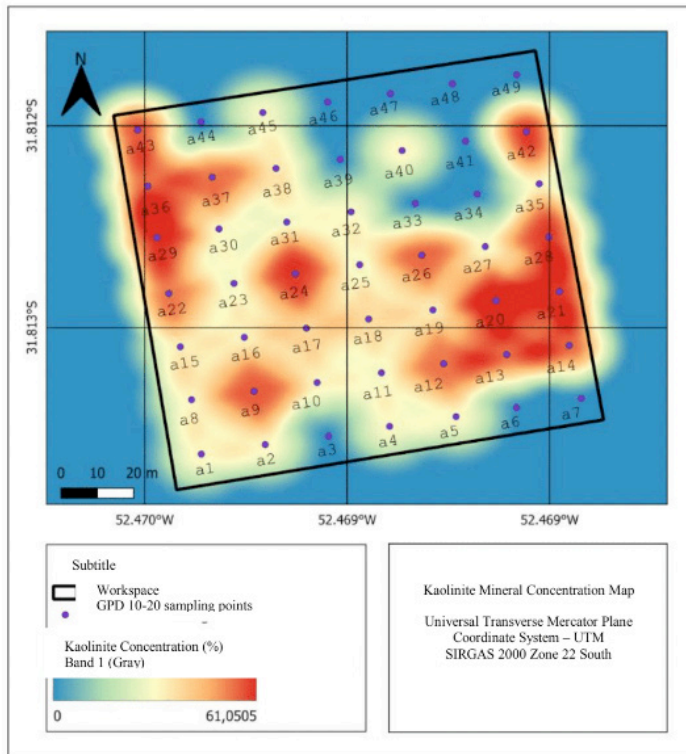
Figure 11 – Distribution map of kaolinite concentrations in the study area.

Source: Author's production.
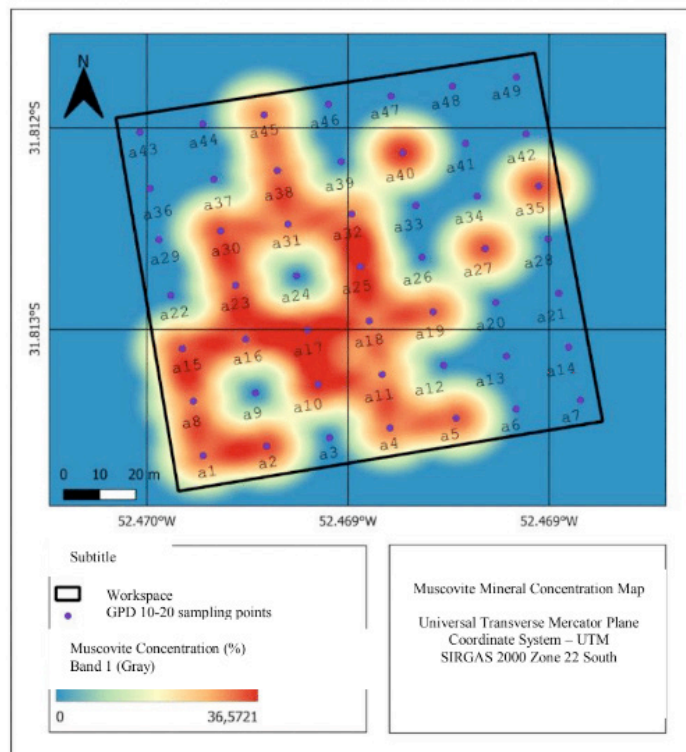
Figure 12 – Distribution map of muscovite concentrations in the study area.

Source: Author's production.
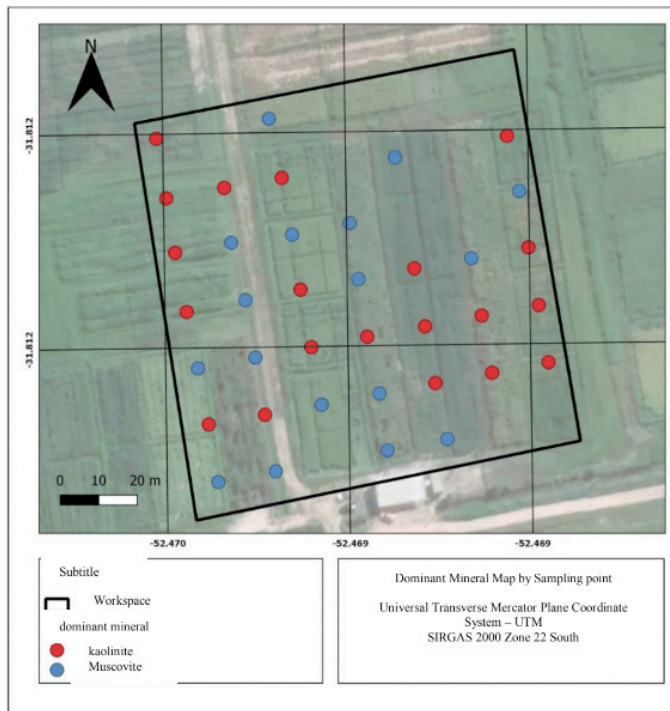
Figure 13 – Map indicating the dominant mineral in each of the analyzed samples. Red symbols correspond to kaolinite dominance and blue symbols correspond to muscovite dominance.

Source: Author's production.

REFERENCES

CARVALHO, E. T. L. (2013). **Avaliação geotécnica de poços de infiltração de águas pluviais.** Tese (Doutorado em Geotecnia), 316p. Universidade de Brasília (UNB), Brasília.

CLARK, R. N., ROUSH, T. L. (1984). **Reflectance spectroscopy: Quantitative analysis techniques for remote sensing applications.** Journal of Geophysical Research: Solid Earth, 89(B7), 6329–6340. doi:10.1029/jb089ib07p06329.

FANG, Q., HONG, H., ZHAO, L., KUKOLICH, S., YIN, K., and WANG, C. (2018). **Visible and Near-Infrared Reflectance Spectroscopy for Investigating Soil Mineralogy: A Review**. Journal of Spectroscopy, 2018, 1–14. doi:10.1155/2018/3168974.

FILIPPINI-ALBA, J. M. F. (2007). **O uso da Espectrorradiometria no Mapeamento de Solos: Estudo de Caso na Estação Experimental Terras Baixas**, 28p. Pelotas: Embrapa Clima Temperado.

FILIPPINI-ALBA, J. M. F., CRUZ, L. E., DUCATI, J. R., DOMINGUES, J. M. M., MORAES, J. O., CUNHA, H. N. (2007). **O uso da Espectrorradiometria no Mapeamento de Solos: Estudo de Caso na Estação Experimental Terras Baixas**, in: OLIVEIRA, R. J. AGRICULTURA EM FOCO: Tópicos Em Manejo, Fertilidade do Solo e Impactos Ambientais - Volume 1 28p. Editora Científica, 191p.

FILIPPINI-ALBA, J.M.; CRUZ, L. E. C.; DUCATI, J. R.; DOMINGUES, J. M. M.; CUNHA, H. N. (2019). **Processing Spectroradiometry data for the simulation of soil physicochemical parameters**. INTERNATIONAL JOURNAL OF DEVELOPMENT RESEARCH, v. 09, p. 28875.

FILIPPINI-ALBA, J. M., FLORES, C. A., MIELE, A. (2020). **Relationships Between A and B/A2 Horizons of Three Soils in the Context of Viticulture**. JOURNAL OF AGRICULTURAL STUDIES, v. 9, p. 440

MENESES, P. R., ALMEIDA, T. (2012). **Introdução ao processamento de imagens de sensoriamento remoto**. Universidade Nacional de Brasília, 277p.

MENESES, P. R., ALMEIDA, T., BAPTISTA, G. M. M. (2019). **Reflectância dos Materiais Terrestres: análise e interpretação**, 39p. São Paulo: Oficina de Textos.

NOVO, E. M. L. M. (2008). **Sensoriamento Remoto: Princípios e Aplicações. 3° edição revista e ampliada**. Editora Edgard Blücher Ltda. São Paulo. 361p.

NGUYEN, T. T., JANIK, L. J., and RAUPACH, M. (1991). **Diffuse reflectance infrared fourier transform (DRIFT) spectroscopy in soil studies**. Australian Journal of Soil Research, 29(1), 49. doi:10.1071/sr9910049

PEREIRA, E. M. (2004). **Estudo do comportamento à expansão de materiais sedimentares da Formação Guabirotuba em ensaios com sucção controlada**. Tese (Doutorado em Engenharia Geotécnica), 253p. Universidade de São Paulo (USP), São Carlos.

PICANÇO, G. A. S. (2019). **Desenvolvimento e análise de um índice ionosférico baseado em dados de conteúdo eletrônico total**. Dissertação (Mestrado em Geofísica Espacial), 195p. Instituto Nacional de Pesquisas Espaciais (INPE), São José dos Campos.

PONTUAL, S., MERRY, N., and GAMSON, P. (2008). **Spectral interpretation field manual. Spectral analysis guides for mineral exploration – GMEX**, 188p. New Zealand: AusSpec International Limited.

SILVA, A. S. A. (2015). **Ferramentas para modelagem e interpolação de dados ambientais em escala regional**. Tese (Doutorado em Biometria e Estatística Aplicada), 121p. Universidade Federal Rural de Pernambuco (UFRPE), Recife.

SOUSA JÚNIOR, J.G.A.; DEMATTÊ, J.A.M. & GENÚ, A.M (2008). **Comportamento espectral dos solos na paisagem a partir de dados coletados por sensores terrestre e orbital**. R. Bras. Ci. Solo, 32:727-738.

SOUSA-JUNIOR, J. G., DEMATTÊ, J. A. M., ROMEIRO-ARAÚJO, S. (2011). **Modelos espectrais terrestres e orbitais na determinação de teores de atributos dos solos: potencial e custos**. Bragantia, 70(3), 610-621.

VISCARRA-ROSSEL, R. A., MCGLYNN, R. N., and MCBRATNEY, A. B. (2006). **Determining the composition of mineral-organic mixes using UV–vis–NIR diffuse reflectance spectroscopy**. Geoderma, 137(1-2), 70–82. doi:10.1016/j.geoderma.2006.07.00.

ZHANG, G.; STRØM, J. S.; BLANKE, M.; BRAITHWAITE, I. (2006). **Spectral Signatures of Surface Materials in Pig Buildings**. Biosystems Engineering, [s. l.], v. 96, ed. 4, p. 495-504, 3 jul. 2006.